Crystal Structure and Iron-Binding Properties of the R210K Mutant of the N-Lobe of Human Lactoferrin: Implications for Iron Release from Transferrins[†,‡]

Neil A. Peterson,[§] Bryan F. Anderson,[§] Geoffrey B. Jameson,[||] John W. Tweedie,[§] and Edward N. Baker*[,§,⊥]

Institute of Molecular Biosciences and Institute of Fundamental Sciences, Massey University, Palmerston North, New Zealand

Received January 20, 2000; Revised Manuscript Received February 28, 2000

ABSTRACT: Lactoferrin (Lf) and serum transferrin (Tf) combine high-affinity iron binding with an ability to release this iron at reduced pH. Lf, however, retains iron to significantly lower pH than Tf, giving the two proteins distinct functional roles. In this paper, we compared the iron-release profiles for human Lf, Tf, and their N-lobe half-molecules Lf_N and Tf_N and showed that half of the difference in iron retention at low pH (∼1.3 pH units) results from interlobe interactions in Lf. To probe factors intrinsic to the N-lobes, we further examined the specific role of two basic residues that are proposed to form a pH-sensitive dilysine trigger for iron release in the N-lobe of Tf [Dewan, J. C., Mikami, B., Hirose, M., and Sacchettini, J. C. (1993) *Biochemistry 32*, 11963−11968] by mutating Arg 210 to Lys in the N-lobe half-molecule Lf_N. The R210K mutant was expressed, purified, and crystallized, and its crystal structure was determined and refined at 2.0-Å resolution to a final *R* factor (R_{free}) of 19.8% (25.0%). The structure showed that Lys 210 and Lys 301 in R210K do not form a dilysine interaction like that between Lys 206 and Lys 296 in human Tf. The R210K mutant retained iron to lower pH than Tf_N, consistent with the absence of the dilysine interaction but released iron at approximately 0.7 pH units higher than Lf_N. We conclude that (i) the ability of Lf to retain iron to significantly lower pH than Tf is due equally to interlobe interactions and to the absence in Lfs of an interaction analogous to the dilysine pair in Tfs, even when two lysines are present at the corresponding sequence positions, and (ii) an appropriately positioned basic residue (Arg 210 in human Lf) modulates iron release by inhibiting protonation of the N-lobe iron ligands, specifically His 253.

Iron is an essential element for animals, but its toxicity and low solubility under physiological conditions require that the levels of free iron be tightly controlled. In animals, this control is achieved by a highly conserved family of proteins known as the transferrins (*1*, *2*), whose archetypal members are transferrin (Tf), the iron transport protein of serum; lactoferrin (Lf), found in the secretory fluids of animals and in white blood cells; and ovotransferrin (oTf) of avian egg white. The transferrins are monomeric glycoproteins of ca. 80 kDa that possess the capacity to bind very tightly, yet reversibly, two ferric ions, together with two synergistically bound carbonate anions.

Crystallographic studies of human Lf (*3*), human serum Tf (*4*), and hen oTf (*5*) have shown that the proteins share essentially the same fold, consistent with their sequence identity of 50−70% (*2*). Each protein comprises two homologous lobes, representing its N- and C-terminal halves, with each lobe further divided into two domains, the N1 and N2 domains in the N-lobe and the C1 and C2 domains in the C-lobe. The iron- and carbonate-binding sites are located within a deep cleft between the domains of each lobe (*3*). Both crystallographic (*6*, *7*) and small-angle X-ray scattering studies (*8*) indicate that iron binding and release by the transferrins are accompanied by substantial conformational changes between the open apo form and the closed iron-bound form. When iron is lost from the N-lobes of Lf and Tf, for example, the N1 and N2 domains move apart through a rigid-body domain rotation of 50−60° that opens the binding cleft (*6*, *7*).

Despite the high level of sequence identity and the similarity of their tertiary structures, individual transferrins differ in their binding properties. Most significant is the much greater acid stability of iron binding by Lf, as compared to that of Tf; human serum Tf loses its iron over the pH range of 6.0 to 4.0, whereas iron release from human Lf occurs in the pH range of 4.0 to 2.5 (*9*). This is consistent with their respective functional roles, in which Tf releases iron to cells in the acidic endosome, whereas Lf retains iron even at low pH, thus protecting against iron-catalyzed free radical formation (*10*) and providing bacteriostatic protection (*11*). Smaller differences are also found between the transferrins of different species and between the two sites of a given protein. Bovine Lf, for example, binds iron more weakly than does

[†]This work was supported by grants from the U. S. Public Health Service (HD20859), the Marsden Fund of New Zealand, and the Health Research Council of New Zealand. E.N.B. also acknowledges research support as an International Research Scholar of the Howard Hughes Medical Institute.

[‡] Atomic coordinates have been deposited with the Protein Data Bank, with accession code 1eh3.

* To whom correspondence should be addressed. Telephone: (+64) 9-373-7599. Fax: (+64) 9-373-7619. E-mail: ted.baker@auckland.ac.nz.

[§] Institute of Molecular Biosciences.

[||]Institute of Fundamental Sciences.

[⊥] Present address: School of Biological Sciences, University of Auckland, Auckland, New Zealand.

10.1021/bi0001224 CCC: $19.00
Published on Web 05/11/2000

FIGURE 1: Polypeptide fold of the recombinant N-lobe of human serum Tf. Side chains of Lys 206 from the N2 domain (upper) and Lys 296 from the N1 domain (lower) are shown in ball-and-stick representation, and the bound iron is shown as a large sphere.

human Lf (*12*) and releases it at slightly higher pH (*13*), and the N-lobe site of serum Tf binds iron more weakly (*14*) and releases it more readily than the C-lobe site (*15*).

These differences must depend on structural variations outside of the primary iron and carbonate coordination spheres, since the same ligands, with the same geometry, are found for both sites of each protein (*2*). Two possible factors have been suggested. First, studies of Lf mutants (*16*) and of the N-terminal half-molecule of human Lf (Lf_N) (*9*) suggest that cooperative interactions from the C-lobe enhance the acid stability of N-lobe iron binding, thereby giving Lf its enhanced overall acid stability. How this is achieved in molecular terms is not known, but there are indications that the terminal helix of the C-lobe is involved (*17*).

A second potential factor is an unusual interdomain interaction between two lysine residues in the N-lobes of Tf and oTf (*18*−*20*). These residues (Lys 206 and Lys 296 in human Tf and Lys 206 and Lys 301 in hen oTf) form a hydrogen-bonded dilysine pair (Figure 1). It has been proposed that charge repulsion resulting from the protonation of this dilysine pair at lowered pH acts as a trigger to stimulate domain opening and iron release (*19*). No such dilysine interaction exists between the equivalent residues (Arg 210 and Lys 301) in human Lf. Instead of interacting with Arg 210, the side chain of Lys 301 adopts a different conformation to form a salt bridge with Asp 297 and with Glu 216 from the other domain (*3*). This localized difference could contribute to the relatively greater acid stability of iron binding by Lf, when compared with that of Tf and oTf (*19*).

The situation is complicated by several Lfs that have two lysine residues at sequence positions corresponding to Lys 206 and Lys 296 in Tf; these include bovine, equine, buffalo, and goat Lfs. At least for bovine, equine, and buffalo Lfs, the proteins have the enhanced acid stability of iron binding that is typical of Lfs, and the crystal structures (*21*−*23*) show that no dilysine pair is formed. The absence of a dilysine pair interaction in the N-lobes of Lfs, even when lysine residues are present at the appropriate sequence positions, signifies a characteristic difference between Lfs and Tfs that could depend either on intrinsic properties of their N-lobes or on the modulating influence of their C-lobes.

Here we report the crystal structure and the iron-binding properties of a mutant of the recombinant N-lobe of human lactoferrin (Lf_N), in which Arg 210 is changed to Lys. This mutation was designed to investigate whether a dilysine pair, such as that in the N-lobe of Tf, would form in the absence of the C-lobe and to assess the contribution of these lysine residues to the intrinsic iron-binding properties of the N-lobe of Lf. We show that a dilysine interaction does not occur in the R210K mutant, analyze the factors that modulate the pH dependence of Tf iron retention, and discuss the implications for the events that are involved in the acid-mediated release of iron from the transferrins.

MATERIALS AND METHODS

Preparation of Recombinant Protein. In vitro site-specific mutagenesis reactions were performed using the method of Kunkel (*24*). A 1005-bp *Eco*RI/*Bgl*II fragment was excised from the 5′ region of the human Lf cDNA and ligated into the *Eco*RI and *Bam*HI sites of M13 mp19. Uracil-containing single-stranded DNA was prepared from this clone, which was then used as a template for oligonucleotide-directed mutagenesis. The clones that contained the R210K mutation were identified by DNA sequence analysis. Restriction digests using *Apa*I and *Sma*I were employed to move a 776-bp fragment of the mutant Lf cDNA from M13 mp19 into the expression construct pNUT-Lf_N. The pNUT-Lf_N plasmid containing the R210K mutation was then transfected into baby hamster kidney cells, and the recombinant Lf was purified from the tissue culture medium by ion-exchange chromatography, as described previously (*9*).

Ultraviolet−*Visible Spectroscopy.* Ultraviolet−visible absorption spectra were recorded from solutions of recombinant transferrins with protein concentrations that ranged between 3.6 and 5.7 mg/mL. Spectra were measured over the range of 250 to 700 nm, using a Hewlett-Packard HP8452A diode array spectrophotometer.

Iron Release Studies. The iron saturation of Lf_N, Tf_N, and the R210K mutant was monitored following dialysis against buffered solutions of varying pH (*9*). The buffers that were used in these studies were 50 mM MES in the pH range of 7.0−5.0 and 50 mM sodium acetate in the pH range of 5.5−3.5. All buffered solutions contained 0.2 M NaCl. Samples were dialyzed for 48 h against each buffer; little change occurred beyond 24 h, but the dialysis was continued for a further 24 h to ensure that the release of iron had essentially reached equilibrium. The proportion of iron-saturated protein was estimated from spectrophotometric measurements of the absorbance at 280 nm, at the wavelength of maximum absorbance for the ligand-to-metal charge-transfer band, λ_{max}

Table 1: Data Processing

space group	*C*2
unit cell	$a = 124.4$ Å
	$b = 57.2$ Å
	$c = 57.3$ Å
	$\beta = 117.1°$
resolution	2.0 Å
R_{merge}[a]	7.3% (26.5%)
I/σ[a]	9.9 (3.2)
no. of unique reflections	23 444
redundancy	2.4
completeness[a]	95.8% (97.1%)

[a] Figures in parentheses for outershell (2.07−2.0 Å).

(450 nm for Lf_N and 472 nm for R210K and Tf_N), and at 700 nm. The absorbance at 700 nm was subtracted from the measurements at 280 nm and at λ_{max} to correct for any background absorbance. The iron saturation of the recombinant transferrins was then estimated from the ratio of the corrected absorbances at 280 nm and λ_{max}. This ratio has a value of ca. 0.045 for iron-saturated Lf_N and ca. 0.0004 for apo Lf_N (*25*).

A curve of best fit was calculated for the pH dependence of iron release from each protein, using an equation that models the ionization of *n* titratable groups (*26*). The pH at which half of the iron has been released corresponds to the apparent pK_a of this ionization process. The differences between the observed iron saturation data and the best-fit curve were minimized by least squares.

Crystallization. Crystallization trials were performed using protein that had been deglycosylated by a mixture of the enzymes endoglycosidase F and peptide N-glycosidase F from *Flavobacterium meningosepticum* (*27*). The deglycosylated protein was prepared for crystallization by concentration to 28 mg/mL in 20 mM HEPES and 1 M NaCl, pH 8.0. Crystals suitable for X-ray diffraction studies were grown by a batch method, by the dropwise addition of 46 μL of the protein solution into 1 mL of water. The crystallizations were then left to slowly equilibrate at 4 °C. Under these conditions, large needlelike red crystals grew over a period of six weeks.

Data Collection and Processing. X-ray diffraction data were collected at 113 K, following the transfer of the crystal into a cryoprotectant solution (crystallization buffer made up in 30% MPD), mounting in a loop, and freezing in a cold nitrogen gas stream. Data were collected with a Rigaku R-axis IIC image plate detector on a Rigaku RU200 rotating anode generator. Profile-fitted intensities were obtained using DENZO and were scaled and merged using SCALEPACK (*28*). Data processing statistics are summarized in Table 1.

Structure Determination. The R210K structure was solved by molecular replacement. The search model was residues 5−319 of the recombinant N-lobe of human Lf (*29*) with the side chain of Arg 210, the ferric and carbonate ions, and all water molecules removed. Molecular replacement was performed using AMoRe (*30*). The rotation and translation functions were calculated using 95% of the data in the resolution range of 8−4 Å and gave a single clear solution that had an *R* factor of 36.6% and a correlation coefficient of 55.2%.

Refinement. Crystal structure refinement was performed using the program XPLOR (*31*). A random subset of 5% of reflections was selected for the calculation of R_{free}, prior to the initiation of refinement. Rigid-body refinement was performed in which the search model was first treated as one fragment and then as two rigid bodies that represent the N1 and N2 domains. The search models were initially rigid-body refined using the data in the resolution range of 8−4 Å. Subsequent rigid-body refinement, in which the maximum resolution was extended, produced a model with an *R* factor of 40.7% and an R_{free} of 41.4% for the data between 6 and 2.0 Å.

Table 2: Structure Refinement

resolution limits	6.0−2.0 Å
no. of reflections	21 459 (1089)
R factor (R_{free})	19.8% (25.0%)
model atoms	
protein residues	4−327
ions	Fe^{3+}, CO_3^{2-}
solvent molecules	170
Average temp. factors (Å^2)	
protein mainchain atoms	17.2
protein side chain atoms	18.3
ordered solvent molecules	21.5
rms deviation from ideal geometry	
bond distances	0.010 Å
bond angles	1.52°
dihedral angles	23.9°

Electron density maps were calculated from the rigid-body refined model, and the Fe^{3+} and carbonate ions were built into the difference electron density. To reduce model bias, selected atoms in the region of the mutation site (residues 301−303 and the side chains of residues 210 and 216) were omitted from the initial refinement. The individual atomic positions and temperature factors of this model were refined by XPLOR, with simulated annealing (*32*), after which time the omitted atoms and the Lys 210 side chain were rebuilt into difference electron density maps. The model was further improved by subsequent rounds of restrained least-squares refinement and simulated annealing, followed by model rebuilding using TURBO FRODO (*33*). Ordered solvent molecules, all modeled as water, were progressively added at locations where there was spherical $|F_o|-|F_c|$ density greater than 3σ above the mean, and there were potential hydrogen-bonding contacts with the neighboring structure. The iron−ligand bonds were initially restrained to conform to standard bond distances, but these restraints were removed from the later rounds of refinement.

The refinement statistics for the R210K model are given in Table 2. The refined model complies well with the observed X-ray diffraction data. The structure has good overall stereochemistry, with a root-mean-square (rms) deviation of 0.01 Å from standard bond lengths and an rms deviation of 1.5° from standard bond angles. A Ramachandran plot (*34*) of the mainchain torsion angles shows that 87.2% of nonglycine and nonproline residues are within the most favored regions of conformational space and that 99.3% are within the allowed regions. Leu 299 is outside of the allowed regions. However, this residue has well-defined electron density and is the central residue of a γ-turn that is conserved in all transferrin structures (*21*).

RESULTS

Iron Binding. The R210K mutant binds iron at neutral pH and exhibits the characteristic red-brown color of iron-bound

Table 3: Iron Binding and Release

	Lf_N	Tf_N	R210K
λ_{max} of charge-transfer band (nm)	450	472	472
no. of iron release data	15	25	19
pH range of iron release	5.0−3.8	6.1−4.7	5.5−4.3
pH at 50% iron saturation	4.34 ± 0.01	5.58 ± 0.04	4.98 ± 0.04

transferrins (*2*). This color is due to a ligand-to-metal charge-transfer band that results from the excitation of an electron from a π orbital of one of the tyrosine ligands into a π^* orbital of the bound iron (*35*). The λ_{max} of this charge-transfer band is significantly red-shifted from 450 in Lf_N to 472 nm in R210K (Table 3). This indicates that the mutation of Arg 210 changes the electronic character of the interactions between the tyrosine ligands and the bound ferric iron.

Iron Release. The recombinant N-lobe of human serum transferrin (Tf_N) releases iron at approximately 1.3 pH units higher than the recombinant N-lobe of human lactoferrin (Lf_N). The iron-bound form of Lf_N is stable above pH 5.0, and iron release is essentially complete at pH 3.8 (Figure 2). In contrast, under identical conditions, Tf_N releases iron over the pH range of 6.1 to 4.7. The pH at which 50% of iron has been released is 4.3 for Lf_N and 5.6 for Tf_N (refer to Table 3).

The mutation of Arg 210 to Lys decreases the stability of iron binding by the N-lobe of lactoferrin in acidic conditions. Half of the iron has been released from R210K at pH 5.0 (Figure 2 and Table 3), which indicates that this mutant releases iron at approximately 0.7 of a pH unit higher than Lf_N. Consequently, the pH dependence of iron release from the R210K mutant is intermediate between those of Lf_N and Tf_N (Figure 2).

Protein Structure. The polypeptide conformation of the R210K mutant is essentially the same as the wild-type Lf_N (*29*). Superposition of R210K onto the Lf_N structure gives an rms difference of 0.81 Å for all main chain atoms in the residue range of 5 to 321. The individual domains superimpose more closely onto Lf_N than does the whole molecule (0.50 Å for N1 and 0.48 Å for N2), which reflects a slight change in the relative orientation of these domains. If the N1 domains of Lf_N and R210K are superimposed, then a rotation of 4.5° is required to match the N2 domains of the two proteins. The movement is primarily a twist of one domain relative to the other, although the domains of R210K are also slightly more closed over the interdomain cleft than the Lf_N domains.

The iron- and carbonate-binding site is represented by well-defined electron density. The bond lengths of the R210K binding site are very similar to those in the Lf_N structure (Table 4), and the slight differences are within the estimated error levels of the structural analyses (approximately 0.1 Å in bond lengths). This indicates that the mutation of Arg 210 does not significantly alter the structure of the iron-binding site of Lf_N.

Mutation Site. The mutation site is located in a well-ordered region of human Lf (*3*). Lys 210 is represented by clearly defined electron density in the R210K structure (Figure 3a) and has an average temperature factor of 12.2 $Å^2$, substantially lower than the average for the whole model (18 $Å^2$). The polypeptide conformation is not affected by the mutation. The only significant structural changes in the region of the mutation site are in the nature of the mutated residue and the locations of ordered water molecules.

The side chain of Lys 210 occupies a similar position in the R210K structure to that of Arg 210 in Lf_N (Figure 3a) and has a conformation that is essentially the same as Lys 206 in human serum Tf. In iron-bound Tf_N, the amino groups of Lys 206 and Lys 296 form the "dilysine trigger" hydrogen bond (*20*). However, Lys 210 and Lys 301 do not interact in R210K, because Lys 301 adopts the same conformation as in Lf_N with its amino group positioned between the carboxyl groups of Asp 297 and Glu 216 (Figure 3d). In this position, the Nζ atom of Lys 301 is 5.8 Å from that of Lys 210. The space that is occupied by the Nζ atom of Lys 296 in Tf_N and the Nη2 atom of Arg 210 in Lf_N is filled by a water molecule in the R210K structure.

The side chain of Arg 210 forms an extensive set of interactions in the native human Lf and Lf_N structures, in a region that is very close to the N-lobe iron-binding site (*29*). These include hydrogen bonds with the phenolate oxygens of Tyr 82 and Tyr 192 and cation−π interactions with the phenolate rings of Tyr 82 and Tyr 92 (Figure 3c). In addition, the Nη2 atom of Arg 210 is only 3.5 Å from the imidazole ring of His 253. The basic Arg 210 side chain would also increase the overall electrostatic potential of this region and hence should stabilize the deprotonated forms of the iron ligands Tyr 92, Tyr 192, and His 253 in the closed form of human Lf.

This local environment is significantly changed by the R210K mutation. The side chain of Lys 210 forms a cation−π interaction with phenolate ring of Tyr 82 (Figure 3d). This interaction is analogous to that between the Arg 210 $N_{\eta 1}$ atom and the phenolate ring of Tyr 82 in wild-type Lf_N. However, several of the other interactions that are formed by Arg 210 in Lf_N are not present in the R210K structure. The Lys 210 side chain does not interact with Tyr 92 or Tyr 192, and it is more than 6 Å from the imidazole ring of His 253, because the position that is occupied by the Nη2 atom of Arg 210 in Lf_N is filled by a water molecule in R210K. The absence of a basic side chain at this location in R210K should decrease the electrostatic potential in the vicinity of the histidine and tyrosine ligands and hence should enhance their susceptibility to protonation.

DISCUSSION

The ability to bind iron tightly, but reversibly, is intrinsic to most of the proposed biological roles of proteins of the transferrin family (*1*). Evolutionary divergence has, however, led to specialized and different roles for Lf and Tf, which is reflected in the ability of Lf to retain iron in significantly more acidic conditions than Tf (*9*). This gives Lf the capacity to scavenge iron that might otherwise catalyze free radical formation or support bacterial growth, whereas Tf can release its bound iron to cells at the reduced intracellular pH (*1*). Here we have sought to identify the structural features that contribute to these differences.

Single-Lobe and Full-Length Proteins. The pH dependence of iron retention by various Lf and Tf species is summarized in Figure 4. Native, full-length serum Tf releases iron over the pH range of 6.0 to 4.0. The release of iron is biphasic, however, with N-lobe releasing at higher pH than the C-lobe (*2*); for human Tf the N-lobe releases iron over the pH range

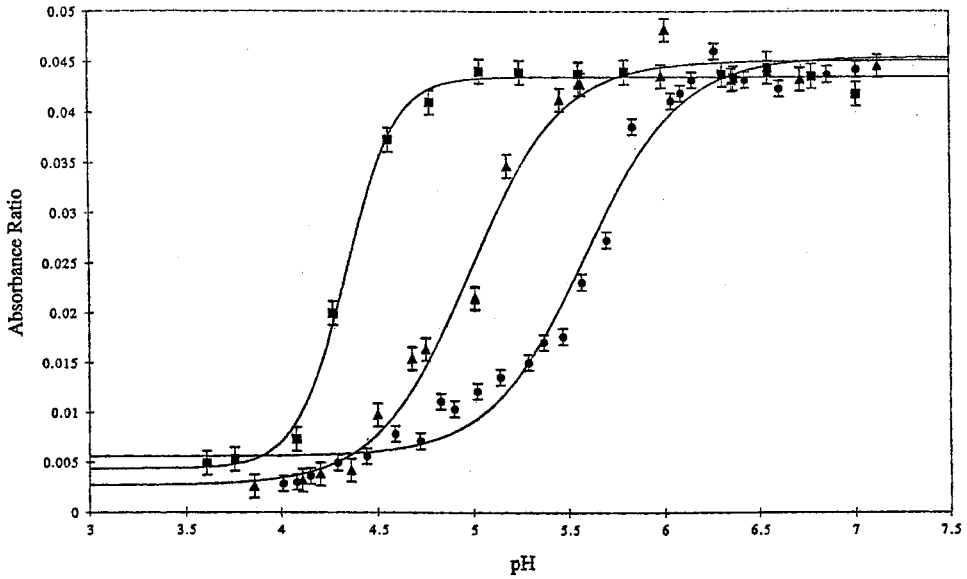

FIGURE 2: pH dependence of iron release from Tf N-lobe half-molecules. Experimental profiles for Lf_N (squares), Tf_N (circles), and the R210K mutant (triangles) are shown, with error bars that indicate the random error associated with the absorbance measurements. Curves were calculated by the least-squares fitting of the observed iron saturation data to an equation that describes the ionization of *n* titratable groups (*26*).

Table 4: Bond Distances at the Iron- and Carbonate-Binding Sites

	Lf_N (Å)	R210K (Å)
$Fe^{3+}\cdots$Asp 60 ($O_{\delta 1}$)	2.0	2.1
$Fe^{3+}\cdots$Tyr 92 (O_{η})	2.0	2.1
$Fe^{3+}\cdots$Tyr 192 (O_{η})	1.9	2.0
$Fe^{3+}\cdots$His 253 ($N_{\epsilon 2}$)	2.2	2.3
$Fe^{3+}\cdots CO_3^{2-}$ (O_1)	2.2	2.2
$Fe^{3+}\cdots CO_3^{2-}$ (O_2)	2.1	2.2
CO_3^{2-} (O_1)$\cdots$Ala 123 (N)	2.8	2.7
CO_3^{2-} (O_2)$\cdots$Arg 121 (N_{ϵ})	2.9	2.8
CO_3^{2-} (O_2)$\cdots$Arg 121 ($N_{\eta 2}$)	2.6	2.7
CO_3^{2-} (O_3)$\cdots$Thr 117 ($O_{\gamma 1}$)	2.6	2.5
CO_3^{2-} (O_3)$\cdots$Gly 124 (N)	3.3	3.1

of 6.0 to 5.5 (*9*) and has a pH_{50} (the pH at which 50% of iron is released) of approximately 5.7−5.8. Under the same conditions, the pH_{50} value for the N-lobe half-molecule Tf_N is 5.6 (Table 3), indicating that the intrinsic properties of the N-lobe of transferrin are not significantly altered by the presence or otherwise of the C-lobe. In marked contrast, both lobes of intact Lf release iron essentially together, with a pH_{50} of approximately 3.0 (*9*). This is significantly lower than the isolated N-lobe half-molecule Lf_N, which has a pH_{50} value of 4.3 (Table 3). Therefore, the presence of the C-lobe enhances the acid stability of iron binding by the N-lobe of full-length Lf by about 1.3 pH units. This stabilization has been noted before (*9*, *16*), and our data suggest that it accounts for about half of the observed difference between Lf and Tf. The mechanism by which interlobe communication occurs in Lf is not clear, but comparisons of the iron-bound and iron-free Lf structures suggest that it may involve contact between the N-lobe and the C-terminal helix (*17*).

Dilysine Pair Region. The N-lobe of Lf evidently also contains features that make its iron binding significantly more stable at low pH than that of Tf, even when removed from the stabilizing influence of interactions with the C-lobe. This is shown by the iron release data; Lf_N has a pH_{50} value of 4.3, which is approximately 1.3 pH units lower than the corresponding figure of 5.6 for Tf_N (Table 3). This provides a measure of the intrinsic difference between the two N-lobes in terms of their acid stability of iron binding.

The dilysine pair interaction between Lys 206 and Lys 296 in human Tf provides a compelling potential explanation for this difference, since no equivalent interaction exists in Lf. The crystal structures of the N-lobes of iron-bound human Tf (*20*), rabbit Tf (*36*), and chicken oTf (*19*) all contain this interaction. The proximity of their Nζ atoms implies that Lys 206 and Lys 296 (human Tf numbering) are hydrogen-bonded and hence that one (or both) of them is not protonated at the crystal pH of ca. 6.0. Presumably, this interaction stabilizes the iron bound form of Tf at higher pH but is destabilizing at lower pH when both residues become protonated, leading to its description as a dilysine trigger (*19*).

In contrast, the equivalent residues (Arg 210 and Lys 301) do not interact either in full-length human Lf (*3*) or in its isolated N-lobe (*29*). Arg 210 occupies a similar position in human Lf to that of Lys 206 in human Tf. However, the more bulky Arg 210 side chain also fills the space that is occupied by the N_{ξ} atom of Lys 296 in human Tf, and the side chain of Lys 301 then adopts a different conformation from that of Lys 296 in Tf to interact with Asp 297 and Glu 216. The latter salt bridge links the two domains and should stabilize the closed form of human Lf in acidic conditions. These interactions in the dilysine pair region are consistent, therefore, with the observed capacity of the N-lobe of human Lf to retain iron at lower pH than that of human serum Tf.

Site-directed mutagenesis experiments confirm the importance of the dilysine pair for the release of iron from the N-lobe of human Tf (*37*−*39*). Although the conditions that have been used by different researchers vary sufficiently to make detailed comparisons of the results difficult, it is consistently clear that the mutation of one or other lysine to disrupt the dilysine pair always retards iron release.

Mutation of Lys 206 to Arg reduces the rate of iron release from the recombinant N-lobe of human serum Tf by approximately 10-fold at pH 5.6 (*37*). This mutation should, as in human Lf, prevent the formation of an equivalent

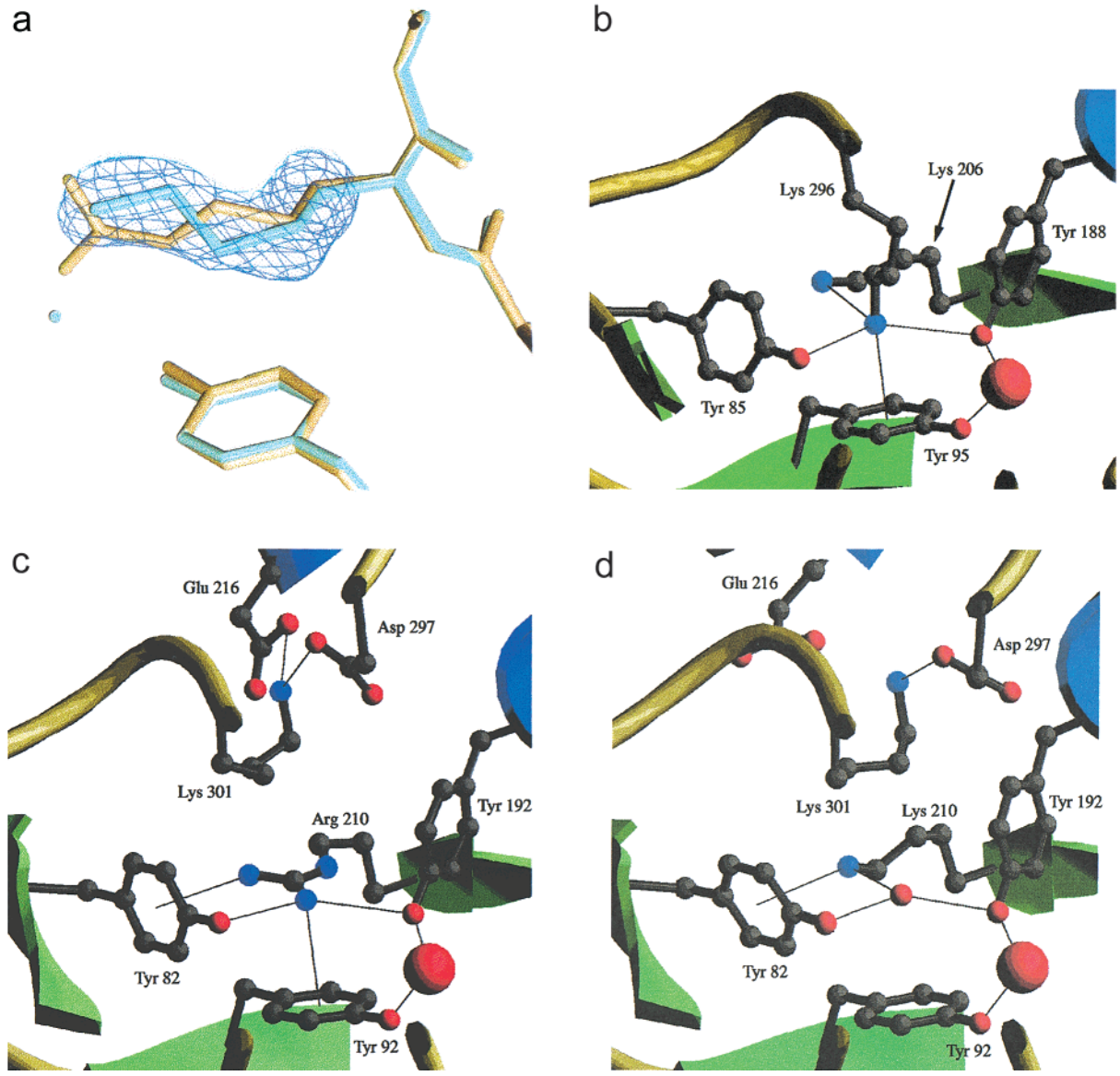

FIGURE 3: Structure in the dilysine pair region. In (a) the conformation of Lys 210 of the R210K mutant (cyan) is compared with that of Arg 210 in wild-type Lf_N (yellow). The $|F_o|-|F_c|$ electron density is shown after simulated annealing refinement with the side chain atoms of Lys 210 omitted from the model. Other panels show the dilysine pair regions of (b) Tf_N, with Lys 206 and Lys 296; (c) Lf_N, with Arg 210 and Lys 301; and (d) R210K, with Lys 210 and Lys 301. Hydrogen bonds and iron−ligand bonds are shown as thin lines, water molecules are shown as small red spheres, and the iron atom is shown as a large red sphere.

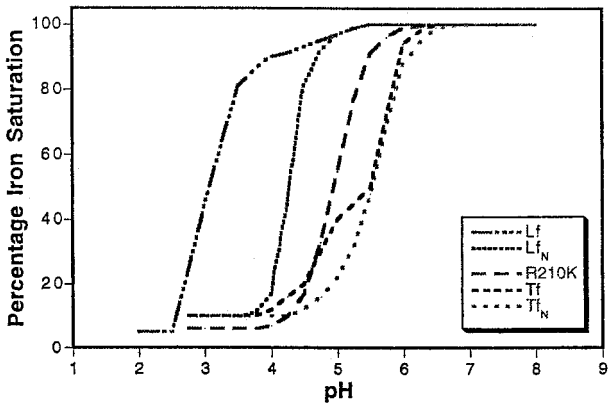

FIGURE 4: pH profiles of iron retention, comparing those for the N-lobe half-molecules Lf_N, Tf_N, and R210K with those for full-length human Lf and human Tf (*9*).

interaction to the dilysine pair because of the greater steric bulk of the arginine side chain. Mutations of Lys 206 or Lys 296 to Ala, which would abolish the dilysine interaction, slow iron release by approximately 250−1000-fold (*38*), and mutations of the lysines to Glu or Gln also have a similar effect, slowing the release of iron by factors of 50−25 000, depending on the conditions (*39*). Note, however, that these are kinetic studies and may reflect other factors in addition to acid stability, possibly including the binding of kinetically significant anions to the dilysine pair (*39*).

Effects of the R210K Mutation. Our mutation of Arg 210 to Lys was designed to examine the structural and functional consequences of having lysine residues at sequence locations that correspond to the dilysine pair of the serum transferrins. This would resemble bovine Lf but set in the background of the N-lobe half-molecule, removed from the influence of the C-lobe.

Two key results have emerged. First, there is no hydrogen-bonded interaction between the two lysines in the R210K mutant, even at the crystal pH of ca. 8.0. Instead of forming

the dilysine pair interaction, the side chain of Lys 301 retains the same conformation that is found in full-length human, bovine, horse, and buffalo Lf and in wild-type Lf_N. In each of these proteins, Lys 301 Nζ sits between the carboxyl groups of Asp 297 and Glu 216 and is 4−6 Å from the basic side chain of residue 210. The observation that the structure in the dilysine trigger region of the R210K half-molecule is the same as in the full-length bovine and horse Lfs shows that it is not the interactions between the N- and C-lobes that prevent the formation of the dilysine pair in the Lfs. Therefore, the lack of a dilysine interaction must be due to the intrinsic properties of the Lf N-lobe.

Second, the presence of two lysine residues does destabilize iron binding by Lf at acid pH but not as much as occurs in serum Tf and for a different reason. The R210K mutant releases iron at approximately 0.7 pH units higher than wild-type Lf_N, as compared with 1.3 pH units higher by Tf_N (Table 3). Thus, the absence of a dilysine interaction in the R210K structure does correlate with an ability to retain iron to lower pH values than Tf_N. The increase in the acid susceptibility of iron release from the R210K mutant, relative to that of Lf_N, is caused by another factor that is related to the Arg to Lys substitution.

Why do Lys 210 and Lys 301 not form a hydrogen-bonded interaction in the R210K mutant of Lf_N, whereas Lys 206 and Lys 296 do in Tf_N? Despite this difference, the dilysine pair regions of the two proteins are remarkably similar. The residues that interact with Lys 206 and Lys 296 in Tf_N are all conserved in human Lf, and conversely those that interact with Lys 210 and Lys 301 in R210K are conserved in human Tf. The only obvious structural feature that correlates with the formation of the dilysine pair interaction is a flip of the 302−303 peptide bond. Residues 301−304 form a type II β-turn (*40*) in diferric human Lf, bovine Lf, and R210K, whereas the corresponding residues in Tf_N, ovoTf, and rabbit Tf adopt the more favorable type I conformation (*40*). There is no clear basis for this correlation, although the peptide flip would produce a subtle change in the electrostatic potential of this region. Modeling suggests that the R210K structure should allow Lys 301 to adopt the same conformation as Lys 296 in human Tf and to form a dilysine interaction with Lys 210. Conversely, Lys 296 in Tf should be able to adopt the conformation of Lys 301 in Lf to interact with Asp 292 and Glu 212, which are conserved in both the Tfs and the Lfs. We conclude that at least two potentially stable conformations are available for Lys 296 in Tf and for Lys 301 in Lf and that these lysine residues simply adopt the conformation that has the lowest energy in each protein, which is determined by differences that we cannot establish at present.

Interactions with the Iron Ligands. Why does the R210K substitution destabilize iron binding in human Lf, even in the absence of a hydrogen-bonded interaction with Lys 301? The crystal structure indicates that the overall polypeptide conformation and the iron-binding site of R210K are essentially the same as in Lf_N. However, the mutation does change the local interactions in the region of the mutation site. The side chain of Arg 210 in wild-type Lf_N forms a cation−π interaction with the phenolate ring of Tyr 92 and a hydrogen bond with the phenolate oxygen of Tyr 192 (Figure 3c). In addition, the Arg 210 $N_{\eta 2}$ atom forms a nonbonded contact with the imidazole ring of His 253. In contrast, in R210K, the side chain of Lys 210 does not interact with either Tyr 92 or Tyr 192 and is remote to the imidazole ring of His 253, because a water molecule occupies the position of the $N_{\eta 2}$ atom of Arg 210 in Lf_N (Figure 3d). The absence of a cationic group adjacent to Tyr 92, Tyr 192, and His 253 should make this set of ligands more susceptible to protonation and thus could account for the observation that R210K releases iron at a higher pH than Lf_N. This weakening of iron binding at low pH is probably a feature of all Lfs that have two lysines at positions 210 and 301, including bovine, horse, buffalo, and goat Lfs.

The presence of a basic side chain adjacent to the histidine and tyrosine ligands seems to be a feature of most serum Tfs. In Tf_N, for example, Lys 296 Nζ occupies a position only 0.5 Å from that of Arg 210 Nη2 in Lf_N and makes highly analogous interactions with the iron ligands (Figure 3b). The importance of basic residues in this region also explains why the K206A/K296A double mutant of Tf releases iron faster than either of the single mutants (*38*); not only will it have no dilysine pair interaction, but it also has no basic side chain to reduce the susceptibility of the histidine and tyrosine ligands to protonation.

Protonation Events in Iron Release. Human Lf and human Tf contain a number of sites where protonation could potentially destabilize the iron-bound form of the proteins. The first is the synergistically bound carbonate anion. Both kinetic studies (*41*) and the crystal structure of Tf_N (*20*) indicate that protonation of the carbonate ion is an early step in iron release, and the crystal structure suggests that this is because bicarbonate interacts more weakly with both metal ion and protein.

There are several possible sites for further protonation events following the formation of bicarbonate. The most obvious is the dilysine pair, whose importance is demonstrated by the large reduction in the rate of iron release that results when one or other of these side chains is removed by site-specific mutagenesis (*38*, *39*). However, both kinetic studies (*41*) and the principle of microscopic reversibility suggest that the protonation of one or more of the iron ligands should also be considered.

The principle of microscopic reversibility states that the reaction pathway for the reverse of a reaction at equilibrium is the exact opposite of the pathway for the forward direction (*26*) and that the transition states for the forward and reverse reactions are identical. A number of events have been implicated in the uptake of iron by the transferrins (*2*). The initial steps involve the attraction of carbonate (or bicarbonate, depending on the pH) into the interdomain cleft (*2*), followed by specific binding to the anion site (*42*). This is followed by the binding of iron to the anion and tyrosine ligands, which are located together on the N2 domain in the open form of the protein (*6*). Such an intermediate species has been demonstrated in the crystal structure of a ferric−nitrilotriacetate complex of the N-lobe half-molecule of oTf (*43*). The binding process would then be completed by the rotation of domain 2 to close the interdomain cleft, which would allow the aspartate and histidine ligands to coordinate to the iron.

If the histidine coordinates to the iron after the tyrosine ligands during iron uptake, then the principle of microscopic reversibility suggests that the histidine ligand should dissociate from the iron before the tyrosines during iron release.

Since the protonated form of imidazole cannot act as a ligand, protonation of His 253 would disrupt the iron−histidine bond, weaken the interactions between the bound iron and the N1 domain, and substantially lower the stability of the iron-bound form of the proteins. A model for the kind of 5-coordinate species that would result from protonation of His 253 is provided by the crystal structure of the H253M mutant of Lf_N (*43*). In this mutant, Met 253 does not coordinate to the iron, and the acid stability of iron binding is greatly reduced. The next steps in iron release would then involve the opening of the binding cleft to produce an intermediate species with the iron bound to the anion and tyrosine ligands on domain 2 only, followed by the loss of iron.

CONCLUSIONS

The enhanced acid stability of iron binding by Lf, relative to Tf, is shown to result from two factors of approximately equal importance, i.e., the stabilizing effect of cooperative interactions from the C-lobe and the lack of an interaction equivalent to the dilysine pair in Tf. The presence of two lysine residues at the appropriate positions in the Lf amino acid sequence does not lead to a dilysine interaction, either in the full-length Lfs (bovine, horse) or in the N-lobe half-molecules (R210K), even though the interaction is sterically feasible. However, the Arg to Lys subsitution does weaken iron binding at low pH, because the loss of a basic group in the immediate vicinity of the tyrosine and the histidine enhances their susceptiblity to protonation. This may also be a feature of other "two-lysine" Lfs, such as bovine, horse, buffalo, and goat Lfs. Finally, the protonation of the histidine ligand, which should be more basic in R210K than in Lf_N, appears to be an important step in the release of iron. The current structural, thermodynamic, and kinetic evidence suggests that a series of protonation events progressively destabilize the iron coordination and/or the closed holo structure. The initial step is the protonation of the synergistic carbonate anion. This is probably followed by the protonation of the pH-sensitive dilysine pair in the N-lobe of serum Tfs. However, in the absence of a dilysine trigger interaction, the second step is probably the protonation of the histidine ligand. The principle of microscopic reversibility then suggests that the next steps would involve the opening of the interdomain cleft, followed by the release of iron.

ACKNOWLEDGMENT

We gratefully acknowledge Ross MacGillivray (University of British Columbia, Vancouver, Canada) for providing the pNUT vector and baby hamster kidney cells, Anne Mason for providing the recombinant N-lobe of human serum transferrin, and Heather Baker, Steve Shewry, Phil Jeffrey, and other colleagues at Massey University for help and encouragement.

REFERENCES

1. Brock, J. H. (1985) in *Metalloproteins* (Harrison, P., Ed.) pp 183−262, MacMillan, London.
2. Baker, E. N. (1994) *Adv. Inorg. Chem. 41*, 389−463.
3. Anderson, B. F., Baker, H. M., Norris, G. E., Rice, D. W., and Baker, E. N. (1989) *J. Mol. Biol. 209*, 711−734.
4. Bailey, S., Evans, R. W., Garratt, R. C., Gorinsky, B., Hasnain, S., Horsburgh, C., Jhoti, H., Lindley, P. F., Mydin, A., Sarra, R., and Watson, J. L. (1988) *Biochemistry 27*, 5804−5812.
5. Kurokawa, H., Mikami, B., and Hirose, M. (1995) *J. Mol. Biol. 254*, 196−207.
6. Anderson, B. F., Baker, H. M., Norris, G. E., Rumball, S. V., and Baker, E. N. (1990) *Nature 344*, 784−787.
7. Jeffrey, P. D., Bewley, M. C., MacGillivray, R. T. A., Mason, A. B., Woodworth, R. C., and Baker, E. N. (1998) *Biochemistry 37*, 13978−13986.
8. Grossmann, J. G., Neu, M., Pantos, E., Schwab, F. J., Evans, R. W., Towns-Andrews, E., Lindley, P. F., Appel, H., Thies, W.-G., and Hasnain, S. S. (1992) *J. Mol. Biol. 225*, 811−819.
9. Day, C. L., Stowell, K. M., Baker, E. N., and Tweedie, J. W. (1992) *J. Biol. Chem. 267*, 13857−13862.
10. Baldwin, D. A., Jenny, R. R., and Aisen, P. (1984) *J. Biol. Chem. 259*, 13391−13394.
11. Bullen, J. J., Rogers, H. J., and Leigh, L. (1972) *Br. Med. J. 1*, 69−75.
12. Aisen, P., and Liebman, A. (1972) *Biochim. Biophys. Acta 257*, 314−323.
13. Legrand, D., Mazurier, J., Colavizza, D., Montreuil, J., and Spik, G. (1990) *Biochem. J. 266*, 575−581.
14. Aisen, P., Liebman, A., and Zweier, J. (1978) *J. Biol. Chem. 253*, 1930−1937.
15. Kretchmar, S. A., and Raymond, K. N. (1986) *J. Am. Chem. Soc. 108*, 6212−6218.
16. Ward, P. P., Zhou, X., and Conneely, O. M. (1996) *J. Biol. Chem. 271*, 12790−12794.
17. Jameson, G. B., Anderson, B. F., Norris, G. E., Thomas, D. H., and Baker, E. N. (1998) *Acta Crystallogr., Sect. D 54*, 1319−1335.
18. Baker, E. N., and Lindley, P. F. (1992) *J. Inorg. Biochem. 47*, 147−160.
19. Dewan, J. C., Mikami, B., Hirose, M., and Sacchettini, J. C. (1993) *Biochemistry 32*, 11963−11968.
20. MacGillivray, R. T. A., Moore, S. A., Chen, J., Anderson, B. F., Baker, H., Luo, Y., Bewley, M., Smith, C. A., Murphy, M. E., Wang, Y., Mason, A. B., Woodworth, R. C., Brayer, G., and Baker, E. (1998) *Biochemistry 37*, 7919−7928.
21. Moore, S. A., Anderson, B. F., Groom, C. R., Haridas, M., and Baker, E. N. (1997) *J. Mol. Biol. 274*, 222−236.
22. Sharma, A. K., Paramasivam, M., Srinivasan, A., Yadav, M. P., and Singh, T. P. (1998) *J. Mol. Biol. 289*, 303−317.
23. Karthikeyan, S., Paramasivam, M., Yadav, S., Srinivasan, A., and Singh, T. P. (1999) *Acta Crystallogr., Sect. D 55*, 1805−1813.
24. Kunkel, T. A., Roberts, J. D., and Zakour, R. A. (1987) *Methods Enzymol. 154*, 367−382.
25. Ainscough, E. W., Brodie, A. M., and Plowman, J. E. (1979) *Inorg. Chim. Acta 33*, 149−153.
26. Fersht, A. (1985) *Enzyme Structure and Mechanism*, 2nd ed., W. H. Freeman and Company, New York.
27. Baker, H. M., Day, C. L., Norris, G. E., and Baker, E. N. (1994) *Acta Crystallogr., Sect. D 50*, 380−384.
28. Otwinowski, Z., and Minor, W. (1997) *Methods Enzymol. 276*, 307−326.
29. Day, C. L., Anderson, B. F., Tweedie, J. W., and Baker, E. N. (1993) *J. Mol. Biol. 232*, 1084−1100.
30. Navaza, J. (1994) *Acta Crystallogr., Sect. A 50*, 157−163.
31. Brünger, A. T. (1992) *X-PLOR, Version 3.1, A System for X-ray Crystallography and NMR*, Yale University Press, New Haven, CT.
32. Brünger, A. T., and Rice, L. M. (1997) *Methods Enzymol. 277*, 243−269.
33. Cambillau, C., Roussel, A., Inisan, A.-G., and Knoops-Mouthuy, E. (1996) Bio-Graphics, AFMB-CNRS, Marseille, France.
34. Ramakrishnan, C., and Ramachandran, G. N. (1965) *Biophys. J. 5*, 909−933.
35. Patch, M. G., and Carrano, C. J. (1981) *Inorg. Chim. Acta 56*, L71−L73.
36. Sarra, R., Garratt, R., Gorinsky, B., Jhoti, H., and Lindley, P. (1990) *Acta Crystallogr., Sect. B 46*, 763−771.
37. Zak, O., Aisen, P., Crawley, J. B., Joannou, C. L., Patel, K. J., Rafiq, M., and Evans, R. W. (1995) *Biochemistry 34*, 14428−14434.

38. Steinlein, L. M., Ligman, C. M., Kessler, S., and Ikeda, R. A. (1998) *Biochemistry 37*, 13696−13703.
39. He, Q.-Y., Mason, A. B., Tam, B. M., MacGillivray, R. T. A., and Woodworth, R. C. (1999) *Biochemistry 38*, 9704−9711.
40. Venkatachalam, C. M. (1968) *Biopolymers 6*, 1425−1436.
41. el Hage Chahine, J. M., and Pakdaman, R. (1995) *Eur. J. Biochem. 230*, 1102−1110.
42. Zweier, J. L., Wooten, J. B., and Cohen, J. S. (1981) *Biochemistry 20*, 3505−3510.
43. Mizutani, K., Yamashita, H., Kurokawa, H., Mikami, B., and Hirose, M. (1999) *J. Biol. Chem. 274*, 10190−10194.
44. Nicholson, H., Anderson, B. F., Bland, T., Shewry, S. C., Tweedie, J. W., and Baker, E. N. (1997) *Biochemistry 36*, 341−346.

BI0001224